

Apico–basal inhomogeneity in distribution of ion channels in canine and human ventricular myocardium

Norbert Szentadrassy^a, Tamas Banyasz^a, Tamas Biro^a, Gergely Szabo^a, Balazs I. Toth^a,
Janos Magyar^a, Jozsef Lazar^a, Andras Varro^b, Laszlo Kovacs^a, Peter P. Nanasi^{a,*}

^aDepartment of Physiology, University of Debrecen, P.O. Box 22, H-4012 Debrecen, Hungary

^bDepartment of Pharmacology and Pharmacotherapy, University of Szeged, P.O. Box 427, H-6701 Szeged, Hungary

Received 24 June 2004; received in revised form 17 November 2004; accepted 18 November 2004

Available online 29 December 2004

Time for primary review 18 days

Abstract

Objectives: The aim of the present study was to compare the apico–basal distribution of ion currents and the underlying ion channel proteins in canine and human ventricular myocardium.

Methods: Ion currents and action potentials were recorded in canine cardiomyocytes, isolated from both apical and basal regions of the heart, using whole-cell voltage clamp techniques. Density of channel proteins in canine and human ventricular myocardium was determined by Western blotting.

Results: Action potential duration was shorter and the magnitude of phase-1 repolarization was significantly higher in apical than basal canine myocytes. No differences were observed in other parameters of the action potential or cell capacitance. Amplitude of the transient outward K⁺ current (29.6±5.7 versus 16.5±4.4 pA/pF at +65 mV) and the slow component of the delayed rectifier K⁺ current (5.61±0.43 versus 2.14±0.18 pA/pF at +50 mV) were significantly larger in apical than in basal myocytes. Densities of the inward rectifier K⁺ current, rapid delayed rectifier K⁺ current, and L-type Ca²⁺ current were similar in myocytes of apical and basal origin. Apico–basal differences were found in the expression of only those channel proteins which are involved in mediation of the transient outward K⁺ current and the slow delayed rectifier K⁺ current: expression of Kv1.4, KChIP2, KvLQT1 and MinK was significantly higher in apical than in basal myocardium in both canine and human hearts.

Conclusions: The results suggest that marked apico–basal electrical inhomogeneity exists in the canine–and probably in the human–ventricular myocardium, which may result in increased dispersion, and therefore, cannot be ignored when interpreting ECG recordings, pathological alterations, or drug effects.

© 2004 European Society of Cardiology. Published by Elsevier B.V. All rights reserved.

Keywords: Ion channels; K-channel; Membrane currents; Membrane potential; Myocytes

1. Introduction

There are well-known differences in the configuration of action potential and density of the underlying transmembrane ion currents between the adjacent layers of the ventricular wall in mammalian myocardium [1,2]. Recent studies demonstrated—in addition to this transmural gra-

dient—the existence of inhomogeneity of ion channel distribution along the apico–basal axis of the heart in rat [3], rabbit [4], and ferret [5], with the concomitant apico–basal asymmetry in action potential duration in rat [6], guinea pig [7], porcine [8], and canine [9] hearts. These results are quite conflicting probably due to large interspecies variations and differences in the experimental techniques applied [10,11].

Several studies indicate that contribution of the various ion currents to repolarization in human ventricular myocardium, including epi–endocardial differences in configuration

* Corresponding author. Tel.: +36 52 416 634; fax: +36 52 432 289.

E-mail address: nanasi@phys.DOTE.hu (P.P. Nanasi).

of the action potential and underlying ion currents, resembles most that observed in canine heart [12–14]; however, no data are available in these tissues regarding apico–basal distribution of ion channels involved in cardiac repolarization. In this study, therefore, we compared densities of the most important ion channel proteins of the conducting pore and some major regulating subunits expressed in the apical and basal regions of the canine and human ventricular wall. In addition, electrophysiological studies were performed to directly measure differences in the underlying ion current densities in canine cells and to reveal possible differences in kinetic properties of the currents. Demonstrating marked apico–basal differences in the amplitudes of canine I_{to} and I_{Ks} , concomitant with the asymmetrical distribution of the underlying channel proteins in dog and human, the present study provides additional new information extending previous data regarding regional inhomogeneity of repolarization.

2. Methods

2.1. Cardiac preparations

Adult mongrel dogs of either sex were anesthetized with intravenous injections of 10 mg/kg ketamine hydrochloride (Calypsolvet)+1 mg/kg xylazine hydrochloride (Rometar). The hearts were quickly removed in deep anesthesia and placed in Tyrode solution, containing (in mM) NaCl 144, KCl 5.6, CaCl₂ 2.5, MgCl₂ 1.2, HEPES 5, and dextrose 11 at pH=7.4. Human ventricular tissues were dissected from 7 undiseased donor hearts stored in cardioplegic solution. The hearts were obtained from general organ donor patients whose semilunar valves were used for transplantation. In cases of both human and canine hearts, approximately 5×5 mm segments were dissected from the apical and the basal regions of the left ventricular free wall—as shown in Fig. 1A—for determination of channel protein density. These samples were frozen and stored in liquid nitrogen until use.

The investigation conforms with the Guide for the Care and Use of Laboratory Animals published by the U.S. National Institutes of Health (NIH Publication No. 85-23, revised 1996), and with the principles outlined in the Declaration of Helsinki. The experimental protocol, applied for human hearts, was also approved by the local ethical committee (No. 51-57/1997 OEJ).

2.2. Electrophysiological studies in canine ventricular myocytes

Single canine myocytes were obtained by enzymatic dispersion using the segment perfusion technique, as described previously [15]. Following digestion of the left ventricular myocardium with 1 mg/ml collagenase (Worthington, Type II) in Joklik solution (Sigma) containing 50 μ M Ca²⁺ for 30 min, portions of the left ventricular wall,

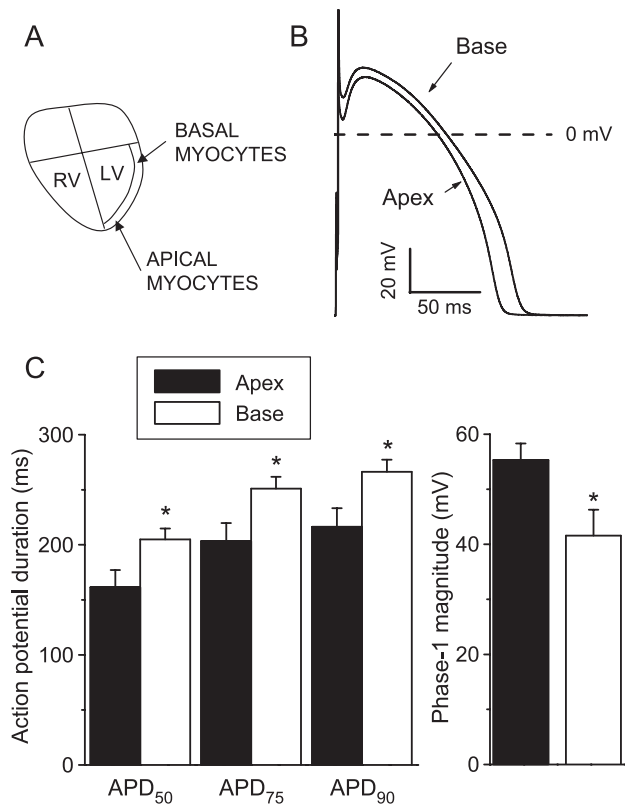


Fig. 1. (A) Schematic diagram showing the origin of apical and basal tissue samples. (B,C) Representative superimposed action potentials and their characteristic parameters recorded from canine left ventricular myocytes of apical and basal origin (each $n=14$). Amplitude of early repolarization (phase-1 magnitude) was measured from the inflection point of the action potential to its overshoot. Columns and bars represent mean \pm S.E.M. values; asterisks denote significant differences ($P<0.05$) between apical and basal myocytes.

having either apical or basal origin (see Fig. 1A), were cut into small pieces and the cells were released from the tissue by gentle agitation. The viable cells were sedimented in a thermoregulated (37 ± 0.1 °C) plexiglass chamber, allowing for continuous superfusion (10 ml/min) with oxygenized Tyrode solution. Whole-cell configuration of the patch clamp technique was used for recording transmembrane ion currents. The electrodes were filled with pipette solution, containing (in mM) K-aspartate 100, KCl 45, MgCl₂ 1, HEPES 5, EGTA 10, K-ATP 3 (for K⁺ current measurements), or KCl 110, KOH 40, TEACl 20, HEPES 10, K-ATP 3, and EGTA 10 (in case of Ca²⁺ current measurement). Ion currents were normalized to cell capacitance, determined in each cell using short (10 ms) hyperpolarizing pulses from -10 to -20 mV. Cell capacitance (140 ± 6 pF) and series resistance (4.0 ± 0.65 M Ω) were compensated before the measurement; the capacitive time constant was 0.5 ± 0.06 ms in average. Experiments were discarded when the series resistance was high or increasing during the experiment. Outputs from the clamp amplifier were digitized at 20 kHz using an A/D converter (Digidata-1200, Axon Instruments) under pClamp 6.0 software

control. Pulse protocols used for measurements of Ca^{2+} and various K^+ currents are described in the appropriate part of the results section. Pulse frequency was 0.2 Hz when measuring I_{Ca} , I_{to} and I_{K1} , 0.1 Hz when recording I_{Ks} , and 0.05 Hz in case of I_{Kr} measurements.

Action potentials were recorded in current clamp mode through the patch pipette (containing internal solution similar to used for K^+ current measurements) in Tyrode solution. The cells were continuously paced through the recording electrode at steady stimulation frequency of 1 Hz using 1-ms-wide rectangular current pulses with suprathreshold amplitude, so as a 1–2 ms gap between the stimulus artifact and the upstroke of the action potential could occur. Action potentials were digitized at 100 kHz.

2.3. Western blotting

Membrane proteins from apical and basal regions of canine ($n=8$) and human ($n=7$) left ventricles were obtained using a method modified after Han et al. [16]. Briefly, tissues were pulverized in liquid nitrogen and suspended in ice-cold Tris–EDTA buffer, containing 20 mM Tris, 1 mM EDTA, and 1:100 dilution of Protease inhibitor cocktail. The latter contained 1 mM 4-(2-aminoethyl)benzenesulfonyl fluoride, 0.8 μM aprotinin, 20 μM leupeptin, 40 μM bestatin, 15 μM pepstatin A, and 14 μM E-64 (all from Sigma-Aldrich). The suspension, after sonication on ice, was centrifuged at $100,000\times g$ for 90 min at 4 °C. The pellet was then resuspended in ice-cold Tris–EDTA buffer containing 2% Triton X-100 (Sigma) and was centrifuged again at $100,000\times g$ for 45 min at 4 °C. Samples were then subjected to SDS-PAGE according to Papp et al. [17]: 8% gels were loaded with equal amounts of 40 μg protein per lane and transferred to nitrocellulose membranes (BioRad). Membranes were incubated with 1:50–1:100 dilution of primary antibodies: rabbit anti-Kv1.4, anti-Kv4.3, anti-Kir2.1, anti- $\alpha_{1\text{C}}$, anti-minK, anti-HERG, and anti-MiRP1 (all from Alomone), and goat anti-KChIP2 and anti-LQT1 (from Santa Cruz Biotech). In the case of the rabbit primary antibody staining, membranes were incubated with an antirabbit ABC kit (Vector Laboratories). In the case of the goat primary antibody labeling, membranes were first incubated with a rabbit antigoat secondary antibody (BioRad) and then with the antirabbit ABC kit. Immunoreactive bands were visualized by an ECL Western blotting detection kit (Pierce) on light-sensitive film. For obtaining negative controls, samples were also probed with primary antibodies preincubated with antigenic (control) peptides. In all cases, the specific staining was suspended by the presence of the control peptide (see Fig. 6). To assess equal loading, nitrocellulose membranes were stripped in 200 ml of 50 mM Tris–HCl buffer (pH 7.5) containing 2% SDS and 0.1 β -mercaptoethanol at 65 °C for 1 h and were reprobed with a mouse anti-cytochrome *C* antibody (Santa Cruz) [17]. Band density was quantified using a GelDoc instrument (BioRad) on films exposed and processed equally. Optical

density values obtained for the samples of basal origin were normalized to those of the apical ones derived from the same heart considering the respective apical values as 100%. Normalized densitometric values of several independent experiments were then averaged and expressed as mean \pm S.E.M.

2.4. Statistics

Results are expressed as mean \pm S.E.M. values. The statistical significance of differences obtained between apical and basal samples was evaluated with Student's *t*-test for paired or unpaired data. Differences were considered significant when *P* was less than 0.05, as indicated in the figures by asterisks.

3. Results

3.1. Action potential characteristics and membrane capacitance

Action potentials were recorded from canine ventricular myocytes of both apical and basal origin in current clamp mode. As shown in Fig. 1B and C, apical action potentials were shorter in duration and displayed more prominent early (phase-1) repolarization than basal ones. At the same time, no significant differences were observed in depolarization (maximum rate of depolarization was 300 ± 22 and 275 ± 23 V/s, action potential amplitude was 140.9 ± 2.0 and 138.2 ± 1.4 mV), or in the magnitude of the resting potential (-82.3 ± 0.4 and -81.3 ± 0.4 mV, N.S., $n=14$, apical versus basal cells).

The cell capacitance (determined in voltage clamp mode) was practically equal in the apical (141 ± 5 pA/pF) and basal (139 ± 7 pA/pF) myocytes (N.S., $n=36$), suggesting that the size of these cells was similar.

3.2. L-type calcium current (I_{Ca})

I_{Ca} was measured at +5 mV using 400-ms-long depolarizations arising from the holding potential of -40 mV. In these experiments, Tyrode solution was supplemented with 3 mM 4-aminopyridine, 1 μM E 4031, and 30 μM chromanol 293B in order to block K^+ currents. The peak current density was not significantly different in the apical and basal myocytes (-5.85 ± 0.76 and -7.17 ± 0.63 pA/pF, respectively, N.S., $n=8$), and no differences were found in the current–voltage relationships taken between -30 and $+50$ mV, suggesting that voltage dependence of activation was not different in the two populations of myocytes.

Voltage dependence of inactivation was determined using test depolarizations to +5 mV following a set of prepulses clamped to various voltages between -55 and $+5$ mV for 500 ms. Similar to activation, no significant differences

were observed when comparing voltage dependence of inactivation: midpoint potential of the steady-state inactivation was -19.7 ± 1.3 and -20.9 ± 1.2 mV, while the slope factor was 4.1 ± 0.26 and 4.4 ± 0.25 mV, respectively, in apical and basal myocytes (N.S., $n=8$).

The time constant of current decay at +5 mV was fitted as a sum of two exponential components. Both the rapid and slow time constants, obtained for inactivation of I_{Ca} in apical and basal cells, were comparable (10.6 ± 0.9 and 46.4 ± 10.5 ms versus 10.0 ± 1.0 and 37.2 ± 3.4 ms, respectively, N.S., $n=8$).

3.3. Transient outward current (I_{to})

I_{to} was activated by depolarizations of 400-ms duration to test potentials ranging from -15 to $+65$ mV, arising from the holding potential of -80 mV and increasing in 10-mV steps. Before each test pulse, a short (5 ms) depolarization to -30 mV was applied in order to inactivate the fast Na^+ current, while Ca^{2+} current was blocked by $5 \mu M$ nifedipine. As shown in Fig. 2A and B, apical myocytes displayed

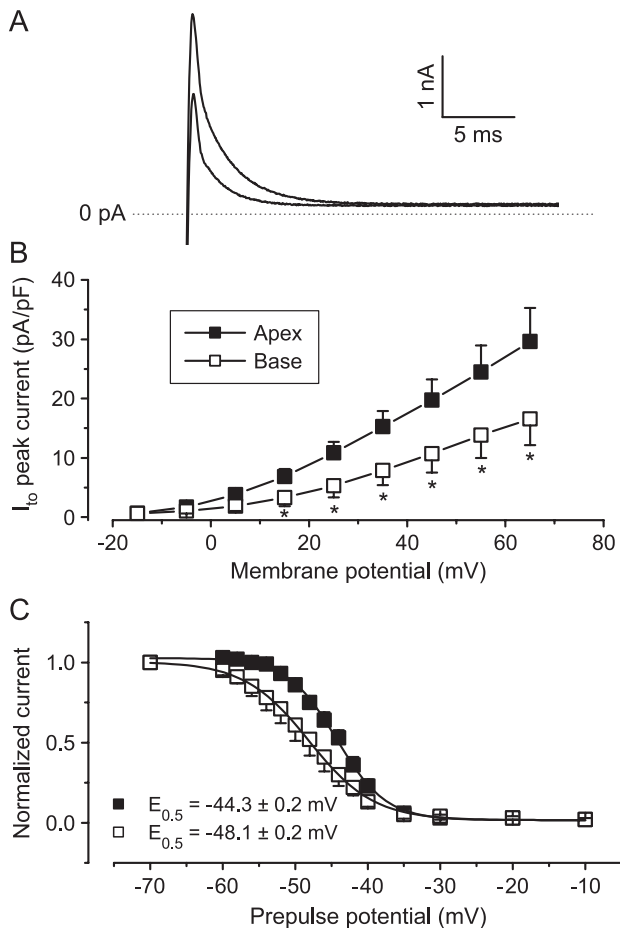


Fig. 2. Properties of the transient outward current in apical and basal canine myocytes (each $n=7$). (A) Representative superimposed I_{to} records taken at $+65$ mV. (B) Current–voltage relationship of peak I_{to} . (C) Voltage dependence of steady-state inactivation of I_{to} . Solid lines were obtained by Boltzmann-fit.

significantly larger peak current density than basal ones at any test potential studied. For instance, the amplitude of I_{to} was 29.6 ± 5.7 versus 16.5 ± 4.4 pA/pF at $+65$ mV in apical and basal cells, respectively ($P < 0.05$, $n=7$).

Voltage dependence of inactivation of I_{to} was determined by a protocol similar to used in the case of I_{Ca} , but I_{to} was tested at $+50$ mV; the holding potential was -80 mV, and the set of prepulses ranged between -70 and -20 mV (Fig. 2C). The steady-state inactivation curve obtained for I_{to} in apical myocytes was shifted by 4 mV to the right comparing to the curve determined for basal cells: the midpoint potential was -44.3 ± 0.2 mV in apical versus the -48.1 ± 0.2 mV value of basal myocytes ($P < 0.05$). In addition, the ‘apical’ curve was slightly, but significantly, steeper than the ‘basal’ one: the slope factor was 3.4 ± 0.15 versus 4.5 ± 0.15 mV, respectively ($P < 0.05$, $n=7$). In contrast to voltage dependence, no significant differences were obtained in the time course of inactivation. The time constant of current decay was 7.2 ± 0.4 ms in apical, and 6.5 ± 0.6 ms in basal myocytes at $+65$ mV (N.S., $n=7$).

3.4. Inward rectifier K^+ current (I_{K1}) and the steady-state current–voltage relationship

The steady-state current–voltage relationship of the membrane was obtained in 7 myocytes by applying 400-ms-long test pulses to potentials ranging between -135 and $+65$ mV in the presence of $5 \mu M$ nifedipine (Fig. 3). The negative branch of this I – V curve is determined by the inward rectifier K^+ current, I_{K1} . No significant differences were found in the density of I_{K1} at any membrane potential studied. On the other hand, apical cells produced significantly larger outward currents than basal ones at membrane potentials more positive than $+40$ mV, i.e., in a potential range where both I_{Kr} and I_{Ks} are known to be active.

3.5. Rapid component of the delayed rectifier K^+ current (I_{Kr})

I_{Kr} was activated by sets of 200-ms-long depolarizing pulses clamped to test potentials ranging from -20 to $+40$ mV. I_{Kr} was assessed as tail current amplitudes recorded following repolarization to the holding potential of -40 mV. I_{Ca} and I_{Ks} were suppressed by $5 \mu M$ nifedipine and $30 \mu M$ chromanol 293B, respectively. As shown in Fig. 4A, the amplitudes of the I_{Kr} current tails were not significantly different in the myocytes of apical and basal origin when the current was activated at $+40$ mV; however, within a narrow range of activation voltage (around $+10$ mV), apical tail currents were smaller in amplitude than basal ones. This is clearly shown in Fig. 4B, where the voltage dependence of activation of I_{Kr} was determined by plotting tail current amplitudes against the test potential used to activate the current. These activation curves were fitted to the two-state Boltzmann function, yielding half-activation voltages of $+13.2 \pm 0.6$ and $+8.3 \pm 0.2$ mV, and slope factors of 8.0 ± 0.6

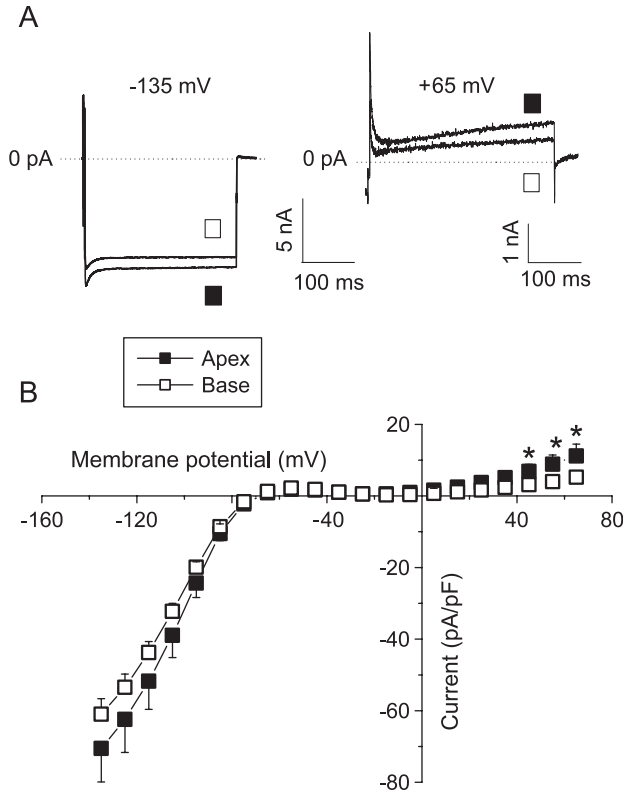


Fig. 3. (A) Representative superimposed inward and outward current records measured at -135 and $+65$ mV, respectively. (B) Current–voltage relationship of the membrane in apical and basal canine myocytes (each $n=7$).

and 6.4 ± 0.2 mV, respectively, in apical and basal myocytes ($P < 0.05$, $n=7$). These results indicate that I_{K_r} requires less positive potentials to activate in basal cells than in apical ones.

Time constant for activation of I_{K_r} was determined using the tail envelope test by applying depolarizations to $+30$ mV with durations continuously increasing from 5 to 900 ms (Fig. 4C). Activation time constants were not different significantly in apical and basal myocytes (58.3 ± 9.8 and 50.9 ± 7.3 ms, respectively, N.S., $n=7$). Deactivation time constants were measured at -40 mV, following activation at $+30$ mV for 200 ms, by fitting the decaying current tails as a sum of two exponential components. No significant differences were seen between the faster (161 ± 23 and 143 ± 15 ms) or slower (3.04 ± 0.45 and 2.6 ± 0.38 s) time constants obtained for deactivation of I_{K_r} in apical and basal cells, respectively (N.S., $n=7$).

3.6. Slow component of the delayed rectifier K^+ current (I_{K_s})

I_{K_s} was evaluated as a fully activated current as well as a tail current shown in Fig. 5A and B. Test depolarizations, arising from the holding potential of -40 mV and having duration of 3 s, were varied from -30 to $+50$ mV. I_{Ca} was inhibited by $5 \mu\text{M}$ nifedipine and I_{K_r} was blocked

using $1 \mu\text{M}$ E 4031. Both the fully activated I_{K_s} (5.61 ± 0.43 versus 2.14 ± 0.18 pA/pF at $+50$ mV) and its tail current (1.65 ± 0.21 versus 0.85 ± 0.19 pA/pF) were significantly larger in apical than in basal myocytes ($P < 0.05$, $n=7$). In addition, no difference in the voltage dependence of activation was observed in the two cell types (Fig. 5C and D).

In contrast to results obtained with I_{K_r} , both time constants (i.e., those estimated for activation and deactivation of I_{K_s}) were significantly shorter in apical than in basal cells. Time constant for activation was determined at $+50$ mV using the tail envelope test by applying depolarizations with duration increasing gradually from 16 to 4000 ms (Fig. 5E). Monoexponential fits yielded time constants of 358 ± 53 ms in apical and 516 ± 34 ms in basal myocytes ($P < 0.05$, $n=7$). Deactivation of I_{K_s} was measured at membrane potentials ranging between -40 mV and $+30$ mV, following activation at $+50$ mV for 3 s, in a similar fashion as was described for I_{K_r} . Deactivation of I_{K_s} was

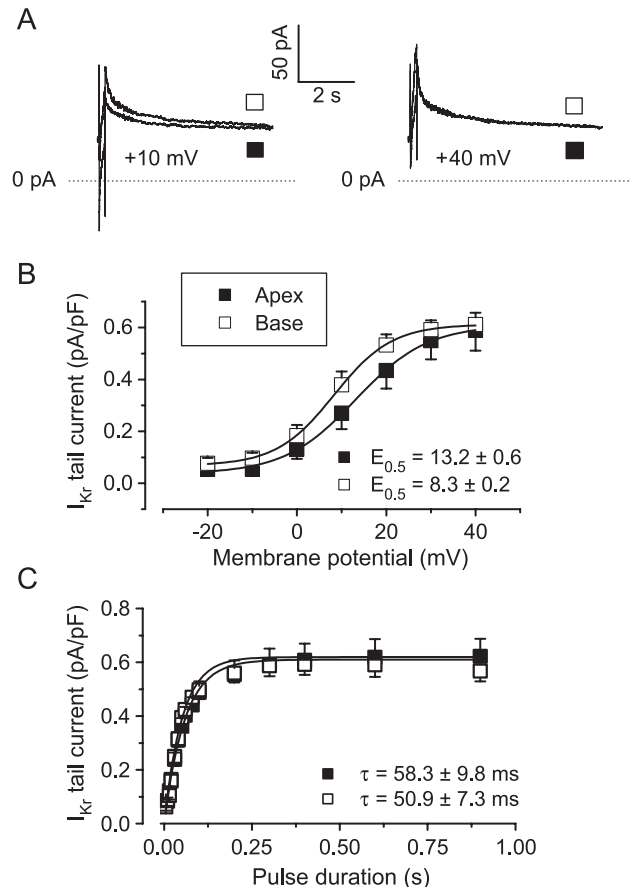


Fig. 4. Properties of the rapid component of the delayed rectifier K^+ current in apical and basal canine myocytes (each $n=7$). (A) Superimposed I_{K_r} tail currents recorded at -40 mV following activation at $+10$ and $+40$ mV for 200 ms (left and right panels, respectively). (B) Voltage-dependent activation of I_{K_r} described by the current–voltage relationship of I_{K_r} current tails. The current was previously activated by depolarization to the membrane potentials plotted in the abscissa. Solid lines were obtained by fitting data to the two-state Boltzmann function. (C) Activation kinetics of I_{K_r} at $+30$ mV determined using the tail envelope test.

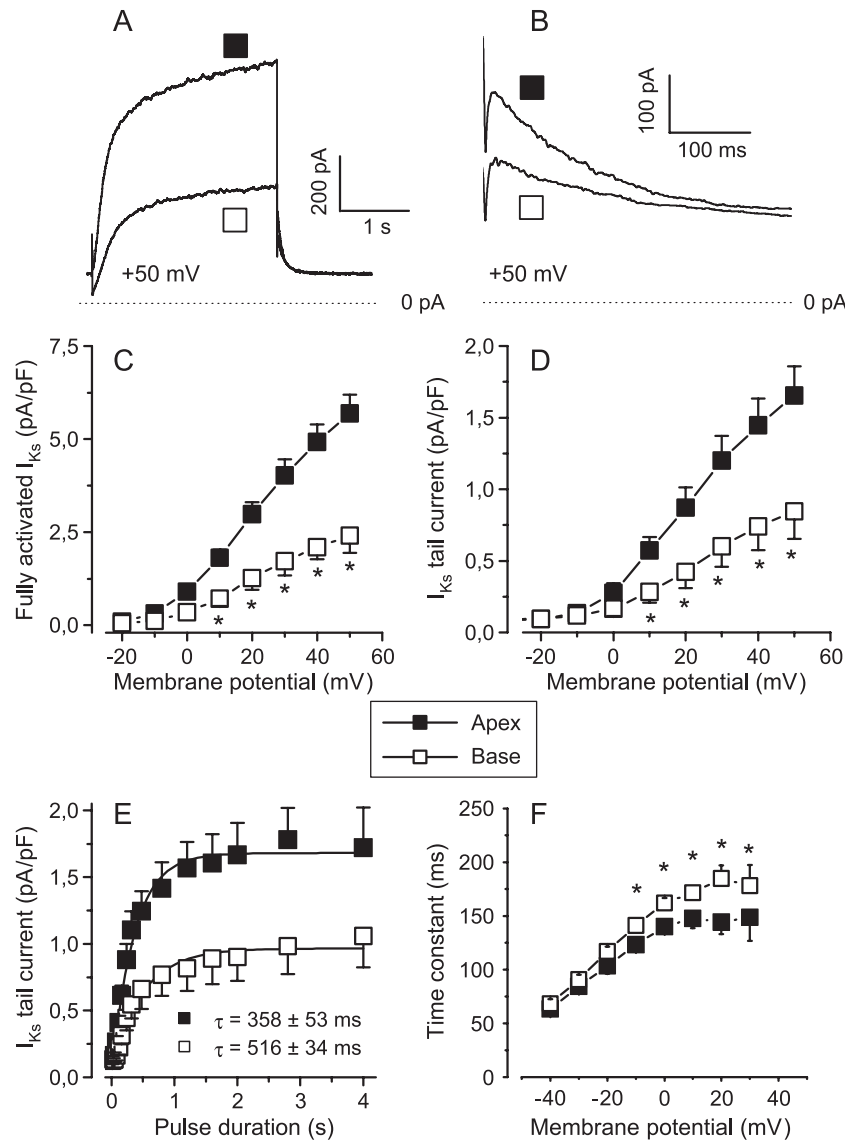


Fig. 5. Properties of the slow component of the delayed rectifier K^+ current in apical and basal canine myocytes (each $n=7$). Representative superimposed fully activated I_{Ks} currents measured at +50 mV (A) and the enlarged I_{Ks} current tails recorded after repolarization to -40 mV (B). Their current-voltage relationships are shown in panels (C) and (D), respectively. (E) Activation kinetics of I_{Ks} at +50 mV determined using the tail envelope test. (F) Voltage dependence of the time constant obtained for deactivation of I_{Ks} .

voltage dependent and followed monoexponential kinetics (Fig. 5F). The time constant was significantly shorter in apical than in basal cells within the voltage range of -10 to +20 mV. For comparison, 144 ± 11 and 185 ± 12 ms values were obtained in apical and basal myocytes, respectively, at +20 mV ($P < 0.05$, $n=7$).

3.7. Apico-basal distribution of ion channel proteins

It was reasonable to test whether the observed apico-basal differences in ion current densities are indeed due to true differences in expression of various channel proteins, or they are consequences of possible damage of ion channels caused by the proteolytic digestion process. Therefore, expression of the underlying channel forming proteins (α -

subunits), together with some of their important regulatory subunits, was compared in pairs of left ventricular myocardial tissue chunks excised from the apical and basal regions of 8 canine hearts. Since our experimental technique allowed only comparison of paired samples—instead of determination of absolute density of channel proteins—the optical densities obtained in basal myocardium were normalized to those measured in apical tissues and expressed as percentage. As is shown in Fig. 6, all applied antibodies reacted specifically with the channel subunits investigated. In addition, we have shown that expression of α_{1C} (pore-forming subunit of L-type Ca^{2+} channel), Kir2.1 (pore-forming subunit of the inward rectifier K^+ channel), as well as HERG and MiRP1 (pore-forming and regulatory subunits of the I_{Kr} channel, respectively) was not signifi-

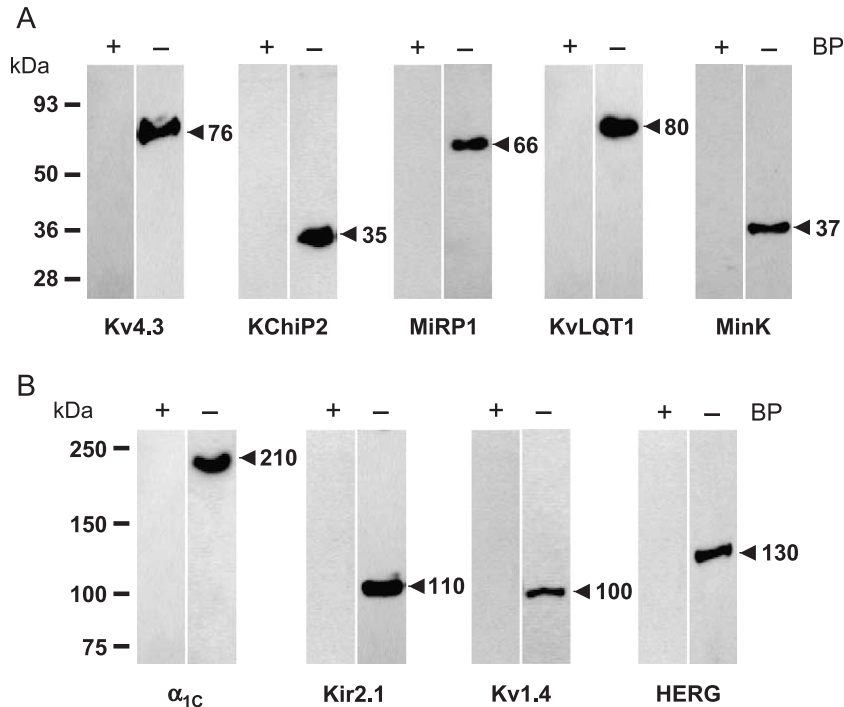


Fig. 6. Expression of ion channel proteins in ventricular myocardium determined by Western blotting. To assess specificity of staining, samples were immunolabeled using appropriate primary antibodies with (+) or without (–) preabsorption with the control blocking peptides (BP). Due to the various molecular weights of the proteins, immunoblots were performed using midrange (A) and high-range (B) molecular weight standards.

cantly different in the apical and basal canine ventricular tissues (Fig. 7A). In contrast, expression of KvLQT1 and MinK (pore-forming and regulatory subunits of the I_{Ks} channel) was significantly less in basal than in apical myocardium. Similar asymmetry was observed in distribution of channel proteins responsible for mediation of I_{to} : the expression of Kv1.4 and KChIP2 (pore-forming and regulatory subunits, respectively) was significantly lower in the basal than in the apical region of the canine heart. The expression of Kv4.3 (another type of pore-forming subunit of I_{to}) was also less in basal than apical tissues; however, this difference failed to reach the level of statistical significance ($P=0.17$ in canine and $P=0.19$ in the human samples).

Results obtained under similar conditions in samples excised from 7 undiseased human hearts are displayed in Fig. 7B. Although quantitative differences in the expression of KChIP2, MinK, and Kv1.4 were observed between dog and human, the pattern of apico–basal asymmetry was similar in the two mammalian species.

4. Discussion

4.1. Apico–basal asymmetry in action potential configuration, ion currents, and channel proteins

Our study is first to systematically demonstrate the presence of marked apico–basal differences in ion currents of canine myocardium and the pattern of ion channel

proteins in both canine and human hearts. The densities of I_{to} and I_{Ks} , currents contributing to ventricular repolarization in most mammalian species, were found to be approximately twice larger in apical than in basal myocytes providing reasonable explanation for the shorter apical action potential.

Among the channel proteins responsible for I_{to} , the expression of Kv1.4 and KChIP2 was significantly lower in basal than in apical myocardium. This seems to be congruent with the apical predominance of I_{to} ; however, it was previously shown that Kv4.3 is the major pore-forming channel subunit in both canine and human ventricular myocardium [18,19]. Therefore, the small apico–basal asymmetry observed in Kv4.3 expression fails to explain the large differences seen in the current. Since the modulatory subunit KChIP2 is known to associate with human and canine Kv4.3 subunits, and coexpression of KChIP2 with Kv4.3 increases the amplitude of I_{to} [20,21], it is plausible to assume that the higher apical expression of KChIP2 may be responsible for the stronger apical I_{to} . Indeed, Rosati et al. [22] came to same conclusions when studying the transmural I_{to} gradient in dog and human, i.e., that the predominantly epicardial expression of KChIP2, rather than that of Kv4.3, may be the reason for the well-documented epi–endocardial asymmetry of the current. An additional indirect support for such a mechanism comes from the study of Yu et al. [23] demonstrating that the amplitude and kinetic properties of I_{to} could be modulated by angiotensin II and losartan without altering the relative expression of Kv4.3 and Kv1.4 subunits. Although we did

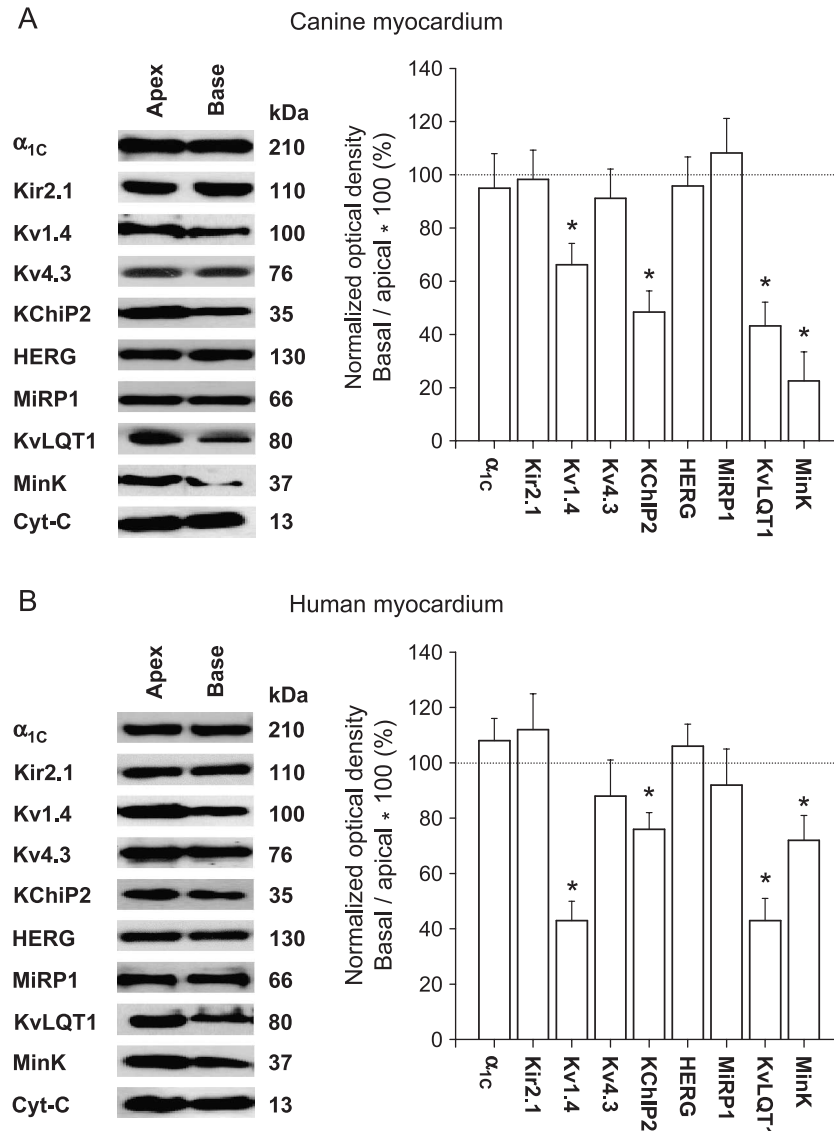


Fig. 7. Apico–basal distribution of ion channel proteins (α -subunits and regulatory proteins) in canine (A) and human (B) ventricular myocardium determined by Western blotting. Series of representative Western blots are presented in left panels. To assess equal loading, nitrocellulose membranes were stripped and reprobed with a mouse anti-cytochrome C antibody (Cyt-C). Average values obtained in 8 canine and 7 human hearts are shown in the right-side diagrams, where relative optical densities (basal normalized to apical) are given in ordinates. Asterisks denote significant differences in apico–basal protein densities.

not measure I_{to} recovery, decrease of Kv1.4 in the basal region can be expected to accelerate reactivation of the current.

The apico–basal asymmetry in I_{Ks} revealed by the electrophysiological measurements in canine myocytes was corroborated by the Western blot studies performed in both canine and human ventricular tissues, since expression of KvLQT1 and MinK (channel proteins involved in mediation of I_{Ks}) was significantly higher in apical than in basal myocardium. Contribution of I_{Ks} to normal repolarization has recently been questioned due to its slow activation kinetics [24,25], whereas it was supported by other studies [26]. Activation of I_{Ks} was faster by 44% in apical than basal canine myocytes, suggesting that activation of this current may accelerate repolarization or

strengthen at least the repolarization reserve in a greater extent in apical cells.

Although no apico–basal differences were obtained in the maximal current density of I_{Kr} (neither in the expression of HERG and MiRP1 proteins), activation of I_{Kr} at 10 mV was weaker in apical than basal myocytes. This relative lengthening, however, seems to be overwhelmed by the more pronounced shortening effects of I_{to} and I_{Ks} in apical cells.

4.2. Comparison with results obtained in other species

Similar to our results, apical action potentials were shorter than basal ones in rat [6], guinea pig [7], and pig [8] hearts. In contrast, others observed the opposite (i.e., that basal action potentials were the shorter) in rabbit [4] and

dog [9]. This latter result, however, was based on measurements of effective refractory periods using needle electrodes *in vivo*, and was restricted to the most superficial subepicardial cell layer. In fact, these authors found no apico–basal gradient in refractoriness in deeper regions of the canine heart [9].

Regarding the apico–basal distribution of individual ion currents responsible for action potential morphology, interspecies differences seem to be even more pronounced. However, there are two exemptions: I_{Ca} and I_{Ks} . I_{Ca} displayed the same apical and basal density in all species studied so far, i.e., in rat [3], guinea pig [7], and dog (this study), while density of I_{Ks} was greater in the apical than in the basal region of the rabbit [4] and canine hearts (this study). We found the density of I_{to} approximately twice larger in apical than in basal canine myocytes, similar to results obtained in rat ventricle [3]. The density of I_{Kr} was greater in apical than in basal rabbit ventricular cells [4], and studied in the epicardial layer of ferret heart, expression of HERG channels (responsible for mediation of I_{Kr}) was apically higher than in the basal region [5]. Clearly contrasting these findings, neither the electrophysiological measurements revealed significant apico–basal differences in the density of canine I_{Kr} , nor the Western blot studies in expression of HERG and MiRP1 proteins in the present work performed in canine and human ventricular myocardium.

4.3. Significance and limitations of the study

In absence of relevant human electrophysiological data, only the Western blot results can be compared directly between dog and human. In general, the apico–basal inhomogeneity was qualitatively similar in the two species, although quantitative differences could be explored in the expression of KChIP2, MinK, and Kv1.4. Based on the results shown in Fig. 7, less apico–basal gradient for both I_{to} and I_{Ks} can be anticipated in human than in dog. Our data suggest that canine heart may be used as a model for studying electrical inhomogeneity in the human heart—but only with limitations. However, considering the large interspecies differences seen in the literature regarding the apico–basal gradient, canine ventricular myocardium still appears to be the best human model in spite of the existing quantitative differences. Since the apico–basal inhomogeneity of repolarization, explored in this study, may result in increased prevalence of cardiac arrhythmias due to increased dispersion under certain (usually pathological) conditions and can modulate efficacy of antiarrhythmic drugs [4,9], present results may extend our basic knowledge and be utilized when developing more effective and rational antiarrhythmic therapy.

There are three types of potential limitations that must be mentioned. First, when measuring the ion currents in canine myocytes, the applied ion channel blockers (e.g., 5 μ M nifedipine or 3 mM 4-aminopyridine) might be insufficient

to block the other currents totally. Since the resulting contamination was presumably similar in both populations of myocytes, the observed apico–basal differences are not likely to be much distorted by this incomplete blockade. Secondly, in our experiments, MiRP1 was recognized by the antibody at a strong band around 66 kDa, which is considerably greater than that identified in previous studies in the literature (25 kDa). The heavier band may be due to posttranslational processing, preferential association between proteins, or antibody association with an epitope located on another protein. This latter possibility cannot be excluded by the antigen-preabsorption response. Thirdly, the number of ion channel subunits involved in ventricular repolarization is much more than has been studied in the present work. In addition, some K^+ channel regulatory subunits (such as MiRP1 or MinK) have recently been shown to combine with various α -subunits. This may distort our results, which, therefore, require careful interpretation.

Acknowledgements

Financial support for the studies was provided by grants from the Hungarian Research Fund (OTKA-T037332, OTKA-T037334, OTKA-T043182), Hungarian Ministry of Health (ETT-06031/2003, ETT-365/2003, ETT-572/2003), and the National Research and Development Programs (NKFP-1A/0011/2002).

References

- [1] Liu DW, Gintant GA, Antzelevitch C. Ionic bases for electrophysiological distinctions among epicardial, midmyocardial, and endocardial myocytes from the free wall of the canine left ventricle. *Circ Res* 1993;72:671–87.
- [2] Stankovicova T, Szilard M, Scheerder ID, Sipido KR. M cells and transmural heterogeneity of action potential configuration in myocytes from the left ventricular wall of the pig heart. *Cardiovasc Res* 2000;45:952–60.
- [3] Bryant SM, Shipsey SJ, Hart G. Normal regional distribution of membrane current density in rat left ventricle is altered in catecholamine-induced hypertrophy. *Cardiovasc Res* 1999;42:391–401.
- [4] Cheng J, Kamiya K, Liu W, Tsuji Y, Toyama J, Kodama I. Heterogeneous distribution of the two components of delayed rectifier K^+ current: a potential mechanism of the proarrhythmic effects of methanesulfonanilide class III agents. *Cardiovasc Res* 1999;43:135–47.
- [5] Brahmajothi MV, Morales MJ, Reimer KA, Strauss HC. Regional localization of ERG, the channel protein responsible for the rapid component of the delayed rectifier K^+ current in the ferret heart. *Circ Res* 1997;81:128–35.
- [6] Shipsey SJ, Bryant SM, Hart G. Effects of hypertrophy on regional action potential characteristics in the rat left ventricle. *Circulation* 1997;96:2061–8.
- [7] Bryant SM, Shipsey SJ, Hart G. Regional differences in electrical and mechanical properties of myocytes from guinea-pig hearts with mild left ventricular hypertrophy. *Cardiovasc Res* 1997;35:315–23.
- [8] Dean JW, Lab MJ. Regional changes in ventricular excitability during load manipulation of the *in situ* pig heart. *J Physiol* 1990;429:387–400.

- [9] Bauer A, Becker R, Karle C, Schreiner KD, Senges JC, Voss F, et al. Effects of the I_{K_r} -blocking agent dofetilide and of the I_{K_s} -blocking agent chromanol 293b on regional disparity of left ventricular repolarization in the intact canine heart. *J Cardiovasc Pharmacol* 2002;39:460–7.
- [10] de Bakker JMT, Opthof T. Is the apico–basal gradient larger than the transmural gradient? *J Cardiovasc Pharmacol* 2002;39:328–31.
- [11] Burton FL, Cobbe SM. Dispersion of repolarization and refractory period. *Cardiovasc Res* 2001;50:10–23.
- [12] Nabauer M, Beuckelmann DJ, Uberfuhr P, Steinbeck G. Regional differences in current density and rate-dependent properties of the transient outward current in subepicardial and subendocardial myocytes of human left ventricle. *Circulation* 1996;93:168–77.
- [13] Li GR, Feng J, Yue L, Carrier M, Nattel S. Evidence for two components of delayed rectifier K^+ current in human ventricular myocytes. *Circ Res* 1996;78:689–96.
- [14] Wettwer E, Amos GJ, Posival H, Ravens U. Transient outward current in human ventricular myocytes of subepicardial and subendocardial origin. *Circ Res* 1994;75:473–82.
- [15] Banyasz T, Magyar J, Kortvely A, Szigeti Gy, Szigligeti P, Papp Z, et al. Different effects of endothelin-1 on calcium and potassium currents in canine ventricular cells. *Naunyn-Schmiedeberg's Arch Pharmacol* 2001;363:383–90.
- [16] Han W, Bao W, Wang Z, Nattel S. Comparison of ion-channel subunit expression in canine cardiac Purkinje fibers in ventricular muscles. *Circ Res* 2002;91:790–7.
- [17] Papp H, Czifra G, Lazar J, Boczan J, Gonczi M, Csemoch L, et al. Protein kinase C isozymes regulate proliferation and high cell density-mediated differentiation of HaCaT keratinocytes. *Exp Dermatol* 2003;12:811–24.
- [18] Akar FG, Wu RC, Deschenes I, Armoundas AA, Piacentino III V, Houser SR, et al. Phenotypic differences in transient outward K^+ current of human and canine ventricular myocytes insights into molecular composition of ventricular I_{to} . *Am J Physiol* 2004;286:H602–9.
- [19] Dixon JE, Shi W, Wang HS, McDonald C, Yu H, Wymore RS, et al. Role of the Kv4.3 K^+ channel in ventricular muscle. A molecular correlate for the transient outward current. *Circ Res* 1996;79:659–68.
- [20] Decher N, Uyguner O, Scherer CR, Karaman B, Yuksel-Apak M, Busch AE, et al. hKChIP2 is a functional modifier of hKv4.3 potassium channels: cloning and expression of a short hKChIP2 splice variant. *Cardiovasc Res* 2001;52:255–64.
- [21] Deschenes I, DiSilvestre D, Juang GJ, Wu RC, An WF, Tomaselli GF. Regulation of Kv4.3 current by KChIP2 splice variants: a component of native cardiac I_{to} ? *Circulation* 2002;106:423–9.
- [22] Rosati B, Pan Z, Lypen S, Wang HS, Cohen I, Dixon JE, et al. Regulation of KChIP2 potassium channel beta subunit gene expression underlies the gradient of transient outward current in canine and human ventricle. *J Physiol* 2001;533:119–25.
- [23] Yu H, Gao J, Wang H, Wymore R, Steinberg S, McKinnon D, et al. Effects of the renin–angiotensin system on the current I_{to} in epicardial and endocardial ventricular myocytes from the canine heart. *Circ Res* 2000;86:1062–8.
- [24] Varro A, Balati B, Iost N, Takacs J, Virag L, Lathrop DA, et al. The role of the delayed rectifier component I_{K_s} in dog ventricular muscle and Purkinje fibre repolarization. *J Physiol* 2000;523:67–81.
- [25] Volders PGA, Stengl M, van Opstal JM, Grlach U, Spatzens RLHMG, Beekman JDM, et al. Probing the contribution of I_{K_s} to canine ventricular repolarization: key role for β -adrenergic receptor stimulation. *Circulation* 2003;107:2753–60.
- [26] Nakashima H, Gerlach U, Schmidt D, Nattel S. In vivo electrophysiological effects of a selective slow delayed rectifier potassium channel blocker in anesthetized dogs: potential insights into class III actions. *Cardiovasc Res* 2004;61:705–14.